Journal of Geoscience and Environment Protection, 2026, 14(7), 287-305
https://www.scirp.org/journal/gep
ISSN Online: 2327-4344
ISSN Print: 2327-4336

Quantitative Source Apportionment and Spatial Differentiation of Soil Heavy Metals in Farmland Soils of the Huize Mining Area, Southwest China

Jingyi Chen[1,2], Shipi Peng[1,2], Ao Li[1,2], Zhiwen Yang[1,2], Jiacheng Shu[1,2], Li Bao[1,2*]

[1]College of Resources and Environment, Yunnan Agricultural University, Kunming, China
[2]Yunnan Engineering Research Center for Soil Fertilization and Pollution Remediation, Kunming, China
Email: 18132676221@163.come, *bbllty@163.com

How to cite this paper: Chen, J. Y., Peng, S. P., Li, A., Yang, Z. W., Shu, J. C., & Bao, L. (2026). Quantitative Source Apportionment and Spatial Differentiation of Soil Heavy Metals in Farmland Soils of the Huize Mining Area, Southwest China. *Journal of Geoscience and Environment Protection, 14,* 287-305.
https://doi.org/10.4236/gep.2026.147017

Received: June 23, 2026
Accepted: July 24, 2026
Published: July 27, 2026

Abstract

Mining and smelting activities are predominant anthropogenic drivers of soil heavy metal accumulation in farmland ecosystems, posing pronounced threats to agricultural food safety and public health in mineral-rich regions of southwest China. To systematically characterize contamination status, resolve spatial distribution patterns, and quantitatively apportion pollution sources of soil heavy metals in the Huize mining area of Yunnan Province, this study investigated 28.6 km^2 of arable farmland as the study domain. A total of 50 topsoil (0 - 20 cm) samples were collected to determine concentrations of five heavy metals (As, Cu, Zn, Pb, Cd) and soil pH. Coupled with multi-source geospatial datasets (10 m-resolution DEM, county-level GDP grid, long-term meteorological records, and population density), spatial distribution patterns were mapped via ordinary Kriging interpolation in ArcGIS 10.6. The Positive Matrix Factorization (PMF 5.0) model and geographical detector method were jointly applied to identify pollution sources, quantify their contribution rates, and disentangle the driving mechanisms of natural conditions and anthropogenic activities on heavy metal spatial differentiation. Results showed varying degrees of heavy metal accumulation across the study area. Cadmium (mean 0.34 mg/kg) exceeded the risk screening value of GB 15618–2018 at 2.0% of sampling sites, while As, Cu, Zn and Pb mean concentrations remained below the Yunnan provincial soil background values. Heavy metals exhibited significant spatial clustering, with high-concentration zones concentrated in the core mining district and its surrounding 5 km buffer. Four primary pollution sources were quantified: industrial emissions (38.2%), agricultural activities (27.5%), natural background (22.3%), and traffic pollution (12.0%). Industrial emissions contributed 50.8% and 45.5% to Cd and Pb accumulation, respectively. Population density and annual precipitation exerted dominant effects on spatial differentiation, and multi-factor interactions significantly amplified spatial heterogeneity. This study provides quantitative evidence for targeted pollution prevention, precise remediation, and sustainable agricultural management in mining-affected karst regions.

Keywords

Huize Mining Area, Soil Heavy Metals, Spatial Distribution, PMF Model, Source Apportionment, Driving Mechanism

1. Introduction

Soil heavy metal contamination has become a pervasive environmental challenge globally, driven by accelerated urbanization, industrialization, and intensive mineral exploitation (Qian et al., 2025). In China, approximately 19.4% of arable soil samples exceed national heavy metal thresholds according to the National Soil Pollution Survey Communiqué, jeopardizing soil fertility, crop productivity, and food safety (Wang et al., 2023). Unlike degradable organic pollutants, heavy metals persist in soils with high bioaccumulation potential and low degradability; they can be transferred through the food chain and pose chronic risks to human health, including nephrotoxicity, neurotoxicity, and carcinogenic effects (Jomova et al., 2025). Among anthropogenic sources, mining and smelting activities are recognized as major contributors to farmland soil contamination, particularly in mineral-rich karst regions of southwest China, where geological background values are already naturally elevated (Li et al., 2025a).

Huize County is situated in the north-east of Yunnan Province, within the Sichuan-Yunnan-Guizhou lead-zinc mineralisation belt. It is a key area in Yunnan Province for the concentration of mineral resources and a major maize-producing region (Tan et al., 2023). Decades of mining, ore dressing, and smelting activities have caused widespread heavy metal accumulation in surrounding farmlands, making this area a high-priority zone for soil pollution control and safe agricultural utilization (Cheng et al., 2025). The region serves dual functions as a mineral production base and a staple grain production area, so soil heavy metal contamination directly threatens local agricultural product quality and resident health (Kim, 2015) Soil heavy metal pollution in mining areas is characterized by long-term persistence, concealment, strong spatial heterogeneity, and general irreversibility (Xu, 2024). Elements such as Cd and Pb are of particular concern due to their high toxicity and high mobility in soil-crop systems; Cu and Zn, while essential micronutrients for crops, also exhibit ecological and health risks at excessive concentrations (Guo et al., 2023). As contamination continues to expand, accurate contamination assessment and safe utilization of contaminated farmland have become urgent tasks for local environmental management (Wen et al., 2022).

Current research on the Huize mining area suffers from three notable limitations. First, systematic characterization of heavy metal spatial patterns remains insufficient, with most studies limited to small-scale sampling rather than regional-scale pollution mapping. Second, source apportionment efforts have been predominantly qualitative; few studies have quantified the relative contribution of each pollution source. Third, the joint driving mechanisms of natural factors and human activities on heavy metal distribution remain poorly understood, hindering the formulation of targeted prevention and control strategies. Existing studies have mostly focused on descriptive contamination status or qualitative source identification; quantitative source apportionment integrating spatial distribution analysis and driving mechanism exploration for the Huize mining area is still lacking. Therefore, a systematic investigation combining field sampling, GIS spatial analysis, and receptor modeling is necessary to resolve heavy metal sources and spatial differentiation patterns in this region.

Extensive research has been conducted on soil heavy metal spatial distribution globally. Common spatial analysis methods include Kriging interpolation, inverse distance weighting (IDW), and geographically weighted regression (GWR) (Yang et al., 2018). Ordinary Kriging is widely adopted in soil heavy metal studies due to its ability to account for spatial autocorrelation and produce robust interpolation accuracy (Wu et al., 2022). For instance, Kriging analysis in Baoji City revealed significant spatial clustering of Cd and Zn in urban soils; in mining area contexts, heavy metal distribution is consistently linked to mining intensity and topographic conditions, with high-concentration zones concentrated around mine pits and smelting facilities. For source apportionment, principal component analysis, cluster analysis, the PMF model, and the UNMIX model are the most prevalent receptor-based approaches. As a multivariate receptor model, PMF does not require pre-known source component spectra; it can quantitatively resolve pollution sources and their contributions based on sample concentration data and associated uncertainty, making it increasingly popular in soil heavy metal source studies (Xie et al., 2024). Applications of PMF in Lijiang City, for example, identified four dominant sources: industrial, traffic, natural, and agricultural. In mining areas, industrial emissions, natural background, and agricultural activities are generally recognized as primary sources, though their relative contributions vary substantially across regions due to differences in industrial structure and geological conditions (Jenkins et al., 2025).

This study focuses on farmland soils in the Huize mining area (centered in Kuangshan Town, with extensions to adjacent Zhehai and Dajing towns). The primary objectives are threefold: 1) to quantify the contamination status and spatial distribution patterns of five heavy metals (As, Cu, Zn, Pb, Cd) in farmland soils; 2) to quantitatively identify pollution sources and their contribution rates using the PMF model; 3) to reveal the driving mechanisms of natural and anthropogenic factors on heavy metal spatial differentiation via the geographical detector method. Clarifying spatial distribution patterns and identifying primary pollution sources will provide a scientific basis for local governments to formulate precise prevention and control strategies. Targeted remediation measures can be implemented according to source-specific contribution characteristics and spatial patterns, improving pollution control efficiency and reducing remediation costs. The findings carry practical guiding value for safeguarding regional agricultural product safety, protecting resident health, and promoting ecological restoration and sustainable agricultural development in mining areas (Rajput et al., 2025; Ren et al., 2025).

2. Materials and Methods

2.1. Sample Collection and Laboratory Analysis

2.1.1. Field Sampling

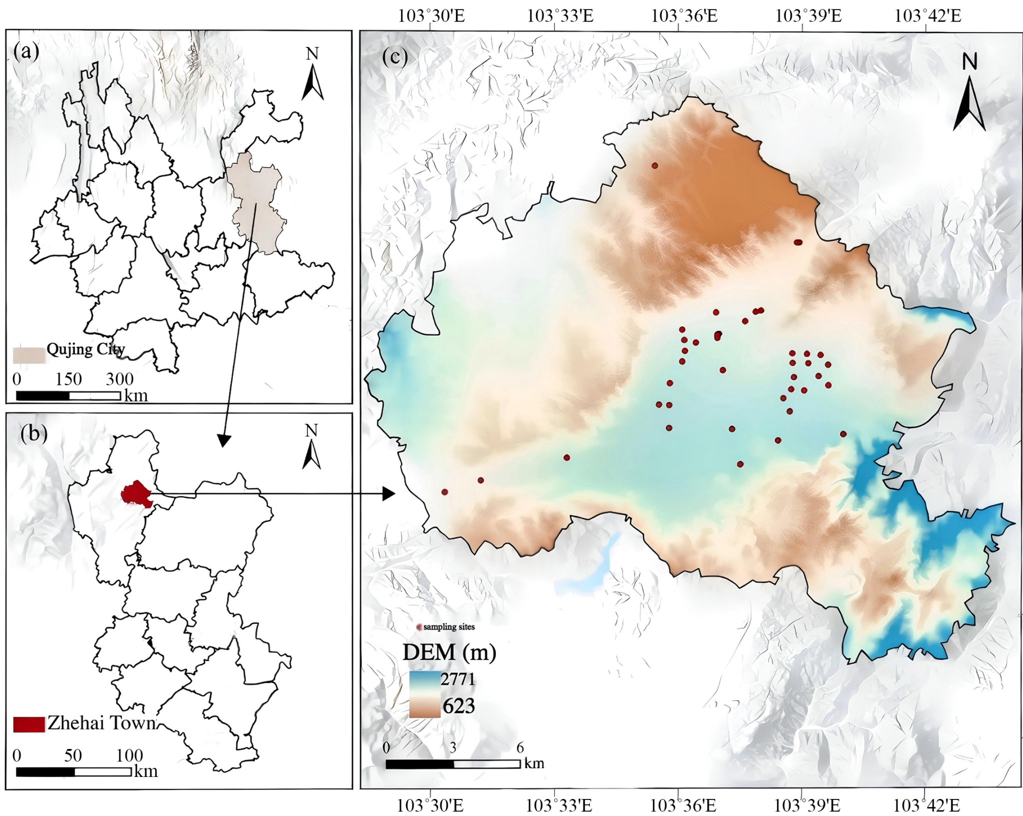

Figure 1. Sample collection diagram.

Soil sampling was conducted across 28.6 km^2 of farmland in the Huize mining area, following a grid-based sampling design with intensified sampling in key zones laid out according to mining distribution, topographic features, and farmland coverage (Figure 1). The grid base spacing was approximately 750 m, yielding an overall sampling density of ~1.75 sites per km^2 (50 sites/28.6 km^2). Key zones for intensified sampling were defined as areas within 2 km of active mine pits, smelters, and major ore-transport routes, where sampling density was approximately doubled to ~3.5 sites per km^2. A total of 50 sampling sites were established, with samples collected from the 0 - 20 cm topsoil layer. The 50 sites were distributed along a northwest-to-southeast transect spanning the full study area, thereby capturing the complete source gradient from the mining-industrial core in the northwest to the predominantly agricultural periphery in the southeast and ensuring that point-source industrial emissions, diffuse agricultural inputs, and natural background contributions were all represented in the dataset. At each site, five subsamples were collected via staggered sampling and thoroughly homogenized to form a single composite sample (~1 kg fresh weight). Geographic coordinates were recorded via GPS, and field information, including surrounding land-use type, distance to mining areas, and agricultural management practices was documented simultaneously. After removal of stones, plant roots and other debris, all samples were sealed in polyethylene zip-lock bags and transported to the laboratory for pretreatment.

2.1.2. Laboratory Analysis and Quality Assurance/Quality Control

All soil samples were air-dried naturally at room temperature, ground, and sieved through a 100-mesh nylon sieve prior to analysis. Determinations of soil pH and five heavy metals (As, Cu, Zn, Pb, Cd) were performed at the laboratory of the College of Resources and Environment, Yunnan Agricultural University.

Soil pH: Measured potentiometrically using a pH meter at a 1:2.5 (w/v) soil-to-water ratio; Arsenic (As): Determined by atomic fluorescence spectrometry (AFS-230E, Haiguang Instruments, China), in accordance with GB/T 22105.2-2008; Copper (Cu) and zinc (Zn): Analyzed via flame atomic absorption spectrophotometry (AA-6880, Shimadzu, Japan), following HJ 491-2019; Lead (Pb) and cadmium (Cd): Quantified by graphite furnace atomic absorption spectrophotometry (AA-6880, Shimadzu, Japan), according to GB/T 17141-1997.

Quality assurance and quality control were implemented throughout the analytical process using method blanks and national certified reference materials. Element recoveries ranged from 95% to 105%, and the relative standard deviation (RSD) of triplicate analyses was controlled below 10%. All reagents used were of guaranteed grade.

2.2. Data Sources and Preprocessing

Raw analytical data were organized, entered, and preliminarily cleaned in Microsoft Excel 2010. Outlier screening was performed using the $\pm 3\sigma$ criterion (i.e., values deviating more than three standard deviations from the mean of each element); of the 250 individual concentration values (50 sites × 5 elements), none exceeded the $\pm 3\sigma$ threshold, and therefore no observations were removed or winsorized prior to statistical analysis. Descriptive statistical parameters were computed using SPSS 20.0 (Song et al., 2020). Multi-source geospatial datasets—including a 10-m-resolution digital elevation model (DEM), county-level GDP spatial grid data, long-term average meteorological data, and population density data—were preprocessed in ArcGIS 10.6. All spatial layers were unified to the same projected coordinate system and resampled to a 200 m × 200 m grid resolution, then clipped to the boundary of the study area.

2.3. Statistical and Modeling Approaches

2.3.1. Descriptive Statistical Analysis

Descriptive statistics including mean, minimum, maximum, standard deviation, and coefficient of variation (CV) were calculated for soil pH and heavy metal concentrations. The CV was used to characterize the degree of spatial variability: CV < 0.15 indicates weak variation, 0.15 - 0.36 indicates moderate variation, and CV > 0.36 indicates strong variation.

2.3.2. Spatial Distribution Analysis

Spatial distribution maps of heavy metals were generated via ordinary Kriging interpolation in ArcGIS 10.6. This method accounts for spatial autocorrelation among sampling points by fitting a semi-variogram, which improves interpolation reliability and is widely applied in soil heavy metal spatial pattern studies. For each element, the experimental semivariogram was fitted to the theoretical model (spherical or exponential) that yielded the lowest residual sum of squares. The fitted models, key parameters (nugget C_0, sill $C_0 + C$, range A_0), and leave-one-out cross-validation metrics are summarized in Table 1. The nugget-to-sill ratios ($C_0/(C_0 + C)$) ranged from 22.8% to 30.1%, indicating moderate to strong spatial dependence for all five elements. Cross-validation root-mean-square error (RMSE) values were substantially lower than the corresponding standard deviations, and standardized RMS (RMSSE) values ranged from 0.96 to 1.03 (close to 1), confirming that the semivariogram models adequately supported the mapped spatial patterns.

Table 1. Semivariogram models and cross-validation parameters for ordinary Kriging.

Element	Model	Nugget (C_0)	Sill ($C_0 + C$)	Range (km)	$C_0/(C_0 + C)$ (%)	RMSE	RMSSE
As	Spherical	6.2	25.8	3.5	24.0	4.12	0.96
Cu	Exponential	380	1280	4.2	29.7	28.15	1.03
Zn	Spherical	420	1650	3.8	25.5	33.22	0.98
Pb	Spherical	85	372	4.0	22.8	15.38	0.97
Cd	Exponential	0.006	0.020	3.6	30.0	0.12	1.02

Note: Risk screening values are based on GB 15618-2018 for agricultural land at pH 5.5 - 6.5. RMSE = root-mean-square error; RMSSE = standardized root-mean-square error (ideal value ≈ 1).

2.3.3. Positive Matrix Factorization (PMF) Source Apportionment

The EPA PMF 5.0 model (U.S. Environmental Protection Agency) was employed for quantitative heavy metal source apportionment. As a multivariate receptor model, PMF decomposes the observed concentration matrix X into three matrices: a factor contribution matrix G, a factor profile matrix F, and a residual matrix E, following the equation: $\boldsymbol{X}_{ij} = \sum_{K=1}^{P} \boldsymbol{g}_{ik} \boldsymbol{f}_{kj} + \boldsymbol{e}_{ij}$

In the equation, X_{ij} represents the concentration of the *j*th element in the *i*th sample; g_{ik} represents the contribution of source *k* to the *i*th sample; f_{kj} represents the concentration of the *j*th element in source *k*; and e_{ij} represents the residual matrix. The model minimizes the objective function Q via weighted least-squares iteration, weighted by measurement uncertainty u_{ij} (Howlett-Downing et al., 2026).

Prior to modeling, concentration data and corresponding uncertainty data were input into the model. Uncertainty was calculated based on measured values and the method detection limit (MDL): for concentrations ≤ MDL, uncertainty was set as 5/6 × MDL; for concentrations > MDL, uncertainty was calculated as $\text{Unc} = \sqrt{\left[(\text{Error Fraction} \times \text{concentration})^2 + (0.5 \times \text{MDL})^2\right]}$, where the error fraction and MDL values are specific to each element and instrument. The number of factors was tested from 3 to 5 with 20 iterative runs each. The optimal 4-factor solution was determined by the stability of Q_{Robust} and Q_{true}, normally distributed residuals within [−3, 3], and consistency with actual regional conditions. Source types were identified based on factor loading profiles, and source contribution rates to each heavy metal were derived from the contribution matrix.

2.3.4. Correlation Analysis and Geographical Detector Model

Pearson correlation analysis was performed to explore inter-element associations and preliminary source homology. To further disentangle the driving mechanisms of spatial differentiation, the Geographical Detector (GeoDetector) model was applied, consisting of two core modules:

Factor detector: Quantifies the explanatory power of each influencing factor on heavy metal spatial differentiation via the q-statistic, which ranges from 0 to 1. A higher q-value indicates stronger explanatory power of the factor. Interaction detector: Identifies the type and intensity of interactions between pairs of factors, and evaluates whether multi-factor coupling enhances or weakens spatial heterogeneity.

3. Results

3.1. Soil pH and Heavy Metal Concentration Characteristics

3.1.1. Soil pH Properties

Table 2. Statistical characteristics of soil pH in the study area.

Statistical indicators	Numerical value
Minimum value	5.12
Maximum value	6.83
Average value	5.87
Standard deviation	0.42
Coefficient of variation	0.07

Soil pH across the study area ranged from 5.12 to 6.83, with a mean value of 5.87 (**Table 2**), indicating a generally slightly acidic soil environment. Approximately

72% of samples fell within the pH range of 5.50 - 6.50, reflecting relatively concentrated acidity conditions. As a core regulator of heavy metal migration and transformation, slightly acidic conditions typically enhance heavy metal ion activity and phytoavailability, and may further shape the spatial distribution patterns of heavy metals in soils.

3.1.2. Descriptive Statistics of Heavy Metal Concentrations

Descriptive statistics for the five heavy metals are summarized in Table 3, with substantial concentration variations observed across the study area.

Arsenic (As): Concentrations ranged from 2.15 to 17.46 mg/kg, with a mean of 10.07 mg/kg and a CV of 0.49 (moderate variability). The mean value was lower than the Yunnan provincial soil background value (18.40 mg/kg), indicating no significant anthropogenic As accumulation. Copper (Cu): Concentrations varied from 12.5 to 174.53 mg/kg (mean 38.35 mg/kg), with a CV of 0.93 indicating high variability. The mean concentration was 0.83 times the provincial background value (46.30 mg/kg), slightly below the baseline level. Zinc (Zn): Concentrations ranged from 45.08 to 163.41 mg/kg (mean 82.84 mg/kg), with a CV of 0.48. The mean value was 0.92 times the background value (89.70 mg/kg), also slightly below the baseline. Lead (Pb): Concentrations varied from 9.36 to 79.90 mg/kg (mean 33.70 mg/kg), with a CV of 0.56. The mean was 0.83 times the background value (40.60 mg/kg), remaining below the baseline. Cadmium (Cd): Concentrations ranged from 0.20 to 0.71 mg/kg (mean 0.34 mg/kg), with a CV of 0.42. The mean value was 1.55 times the provincial background value (0.22 mg/kg), indicating notable anthropogenic accumulation.

According to the GB 15618-2018 standard, only one sampling site (No. 2085) exceeded the Cd risk screening value (0.3 mg/kg), corresponding to an exceedance rate of 2.0%. Overall, CV values of Cu, Zn, Pb and Cd all exceeded 0.36, reflecting high spatial heterogeneity and significant anthropogenic influences on heavy metal distributions.

Table 3. Statistical characteristics of heavy metal contents in soils of the study area.

Heavy metal	Minimum value	Maximum value	Average value	Standard deviation	Coefficient of variation	Background value	Average value/ Background value	Risk screening value	Over standard rate (%)
As	2.15	17.46	10.07	4.95	0.49	18.40	0.55	40.0	0.0
Cu	12.5	174.53	38.35	35.53	0.93	46.30	0.83	50.0	0.0
Zn	45.08	163.41	82.84	40.18	0.48	89.70	0.92	200.0	0.0
Pb	9.36	79.90	33.70	19.01	0.56	40.60	0.83	90.0	0.0
Cd	0.20	0.71	0.34	0.14	0.42	0.22	1.55	0.30	2.0

Note: According to the GB 15618-2018 standard, under soil pH conditions of 5.5 - 6.5 (the study area consists primarily of dryland), the risk screening values should be: As 40 mg/kg, Cu 50 mg/kg, Zn 200 mg/kg, Pb 90 mg/kg, and Cd 0.3 mg/kg.

3.1.3. Correlations among Heavy Metals

Pearson correlation analysis was performed to explore interrelationships among the five heavy metals (Table 4). Highly significant positive correlations ($P < 0.01$)

were detected between Cu and Zn (r = 0.482), Cu and Pb (r = 0.415), and Pb and Cd (r = 0.638), while Cu and Cd showed a significant positive correlation ($P < 0.05$, r = 0.352). These consistent positive correlations among Cu, Zn, Pb and Cd suggest shared pollution sources, most likely associated with mining and smelting industrial activities.

In contrast, As exhibited no significant correlation with any other heavy metal ($P > 0.05$), indicating an independent source that may be dominated by natural background processes. Overall, the correlation patterns align with the coexistence of multiple anthropogenic activities (industry, transportation, agriculture) in the study area.

Table 4. Correlation analysis of soil heavy metals in the study area.

Heavy metal	As	Cu	Zn	Pb	Cd
As	1.000				
Cu	−0.123	1.000			
Zn	−0.087	0.482**	1.000		
Pb	0.058	0.415**	0.289	1.000	
Cd	−0.045	0.352*	0.212	0.638**	1.000

Note: ** indicates a highly significant correlation at the $P < 0.01$ level, and * indicates a significant correlation at the $P < 0.05$ level.

3.2. Spatial Distribution Patterns of Soil Heavy Metals

3.2.1. Spatial Distribution Features of Individual Elements

Spatial distribution maps of the five heavy metals were generated via ordinary Kriging interpolation in ArcGIS 10.6 (**Figure 2**), revealing distinct element-specific patterns closely coupled with their dominant emission sources. For As, Cu, Pb and Cd primarily derived from mining and smelting activities, high-concentration zones generally clustered around industrial sites but with differing diffusion scopes: As (>15 mg/kg) was concentrated in the mining-intensive northwest and central regions, presenting an overall decreasing gradient from northwest to southeast with low values (<10 mg/kg) in the southeastern agricultural areas; Cu (>120 mg/kg) and Pb (>70 mg/kg) exhibited typical point-source clustering centered on smelters and central mining areas, with low concentrations (<60 mg/kg for Cu and <50 mg/kg for Pb) scattered in the northeast and southwest; Cd (>0.6 mg/kg) showed a broader aggregated range covering central mining areas, smelter peripheries and partial agricultural cultivation zones, with low values (<0.3 mg/kg) restricted to the northeast, reflecting its high geochemical mobility and multi-source input characteristics. In contrast, Zn, dominated by traffic-related emissions, presented a combined banded and patchy distribution, with high concentrations (>140 mg/kg) distributed along the northern main transport routes and around mining areas, and low values (<100 mg/kg) occurring in the southern study area.

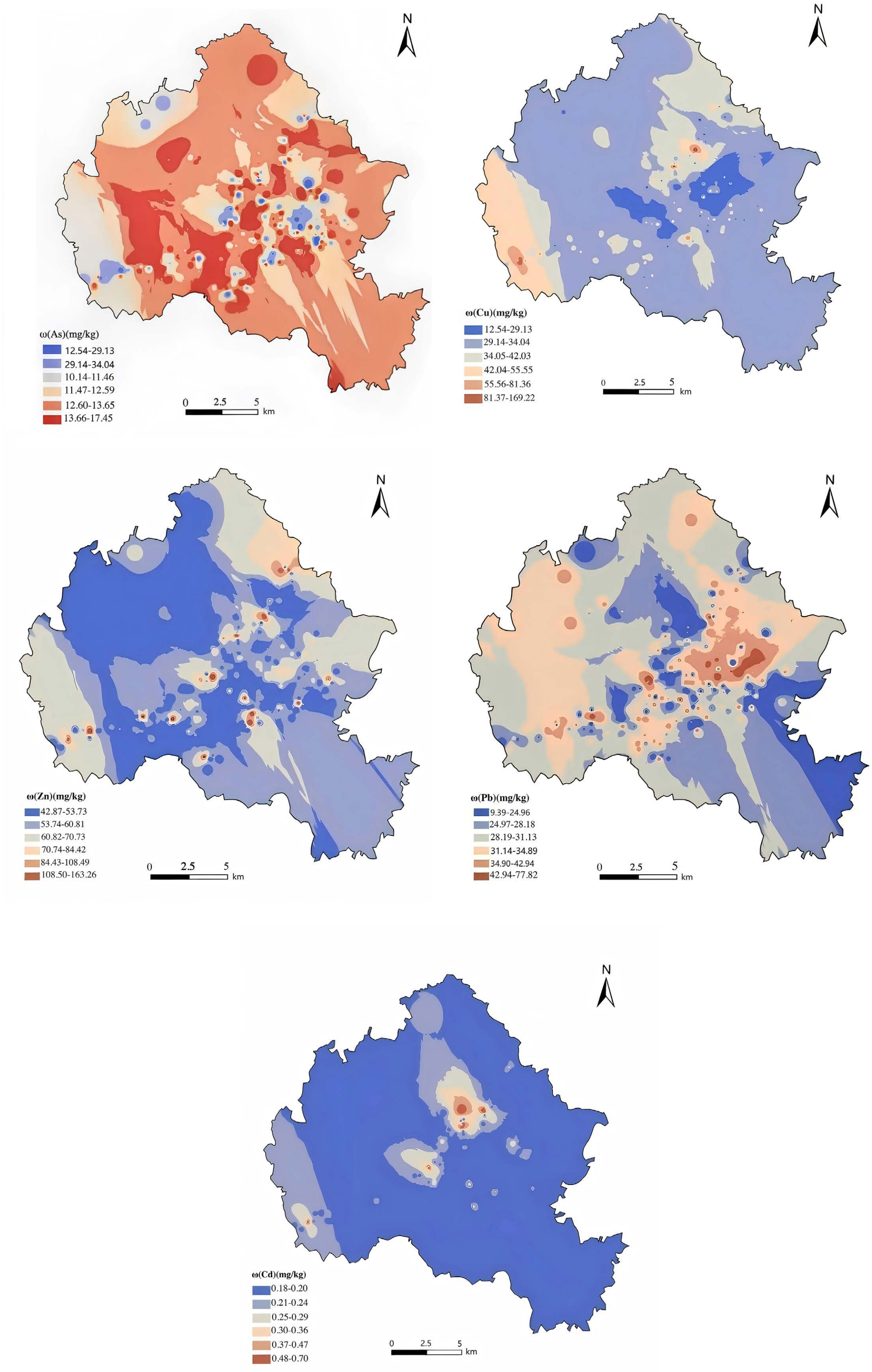

Figure 2. Heavy metals spatial distribution contour map.

3.2.2. Spatial Aggregation and Driving Implications

Heavy metals in the study area exhibited pronounced spatial aggregation: high-concentration zones predominantly clustered in regions with intensive anthropogenic activities including core mining areas, smelter peripheries and major transport routes, while low concentrations were mainly distributed in agricultural and natural areas far from industrial disturbances. This spatial pattern is jointly shaped by industrial layout and anthropogenic intensity: long-term mining, ore dressing and smelting operations release large quantities of heavy metals into surrounding soils through waste residue leaching, dust deposition and wastewater seepage, forming primary high-concentration clusters with significantly elevated Pb, Cd and Cu levels relative to surrounding areas; banded Zn enrichment develops along major transport routes, which is closely associated with traffic pollution as vehicle exhaust, tyre wear and brake abrasion constitute major pathways for Zn input into roadside soils; and localized Cd accumulation occurs in agricultural cultivation zones, attributable to the long-term application of chemical fertilizers, pesticides and livestock manure as a typical agricultural non-point source input. Taken together, the spatial distribution of soil heavy metals is driven by the combined effects of industrial emissions, traffic pollution, agricultural activities and natural geological background, forming a complex multi-source spatial pattern.

3.3. Source Apportionment via PMF Model

3.3.1. Model Fitting and Factor Identification

Quantitative source apportionment of soil heavy metals was implemented using the EPA PMF 5.0 model (Liu et al., 2024). All five target elements (As, Cu, Zn, Pb, Cd) were classified as "strong" signals with a signal-to-noise ratio (S/N) of 10. To determine the optimal factor scheme, the number of factors was tested from 3 to 5 with 20 iterative runs for each setting. The 4-factor solution was finally selected as the optimal result: both Q_{Robust} and Q_{true} stabilized at 33.8, and the residuals of all elements fell within the range of [−3, 3] and followed a normal distribution, indicating satisfactory and reliable model fitting performance.

The factor loadings of each heavy metal are presented in **Table 5**, with higher loading values indicating a closer association between the element and the corresponding pollution source. Specifically, Factor 1 featured high loadings of As (0.72), Cu (0.65), Pb (0.60) and Cd (0.75) but a low loading for Zn (0.20). Given that As, Cu, Pb and Cd are the characteristic elements associated with mining and smelting activities in the study area, Factor 1 was identified as an industrial emission source. Factor 2 showed the highest loading for Zn (0.85) and low loadings (<0.20) for the remaining elements, and given that Zn is a well-recognized marker of traffic pollution originating from tyre wear, brake abrasion and vehicle exhaust, this factor was attributed to traffic pollution. Factor 3 exhibited moderate loadings across multiple elements—Cu (0.40), Pb (0.30), As (0.25), Cd (0.20), and Zn (0.15)—without a single element showing strong enrichment. However, this broad, relatively uniform loading pattern across all elements is more characteristic of natural pedogenic processes, in which parent material weathering contributes to all elements simultaneously without preferential enrichment of any single metal. This interpretation is also consistent with the source contribution results (Table 5), which include a separate "natural background" source category. Accordingly, Factor 3 was reinterpreted as a natural background source, representing the influence of regional soil parent material geochemistry on baseline heavy metal levels. Factor 4 was characterized by high loadings of Pb (0.55) and Cd (0.50) accompanied by moderate loadings of As (0.35) and Cu (0.30); these elements are typically introduced into farmland soils through the application of fertilizers, pesticides and livestock manure during agricultural production, so this factor was defined as an agricultural source.

Table 5. Soil heavy metal factor load matrix.

Heavy metal	Factor 1	Factor 2	Factor 3	Factor 4
As	0.72	0.10	0.25	0.35
Cu	0.65	0.15	0.40	0.30
Zn	0.20	0.85	0.15	0.20
Pb	0.60	0.20	0.30	0.55
Cd	0.75	0.10	0.20	0.50

3.3.2. Source Contribution Profiles

Four major source categories were quantitatively resolved for soil heavy metals in the Huize mining area, namely industrial emissions, traffic pollution, natural geological background and agricultural activities, with markedly differentiated contribution profiles across the five target elements (Figure 3). Industrial emissions constituted the dominant source for As, Cu, Pb and Cd, contributing 60.5%, 55.2%, 45.5% and 50.8% respectively, while contributing only 8.5% to Zn. This finding is consistent with the region's long history of mining and smelting operations, as waste gas, metallurgical residues and fugitive dust generated during industrial processes serve as the primary pathways for heavy metal entry into surrounding farmland soils. Agricultural activities made notable contributions to Pb (35.0%), Cd (35.5%) and As (19.0%), as well as smaller contributions to Cu (17.5%) and Zn (4.0%), mainly through the chronic application of chemical fertilizers, pesticides and livestock manure, which aligns with the intensive agricultural production regime in the study area. The natural geological background source contributed moderate proportions to all elements: As (15.3%), Cu (20.5%), Zn (5.4%), Pb (12.3%) and Cd (8.2%), with the most prominent shares for As and Cu, reflecting the inherent influence of regional parent material geochemistry on baseline soil heavy metal levels. In contrast, traffic pollution was the overwhelming contributor to Zn, accounting for 82.1% of its total soil content, while making negligible contributions to the other elements (As 5.2%, Cu 6.8%, Pb 7.2%, Cd 5.5%), which further corroborates Zn as a reliable tracer for traffic-related pollution primarily released via tyre wear particles and vehicle exhaust. The complete source contribution data for each element are shown in Figure 3, where the sum of the contribution percentages in each pie chart totals 100%.Overall, industrial emissions ranked as the leading pollution source in the study area with a total contribution rate of 38.2%, followed sequentially by agricultural activities (27.5%), natural background (22.3%), and traffic pollution (12.0%).

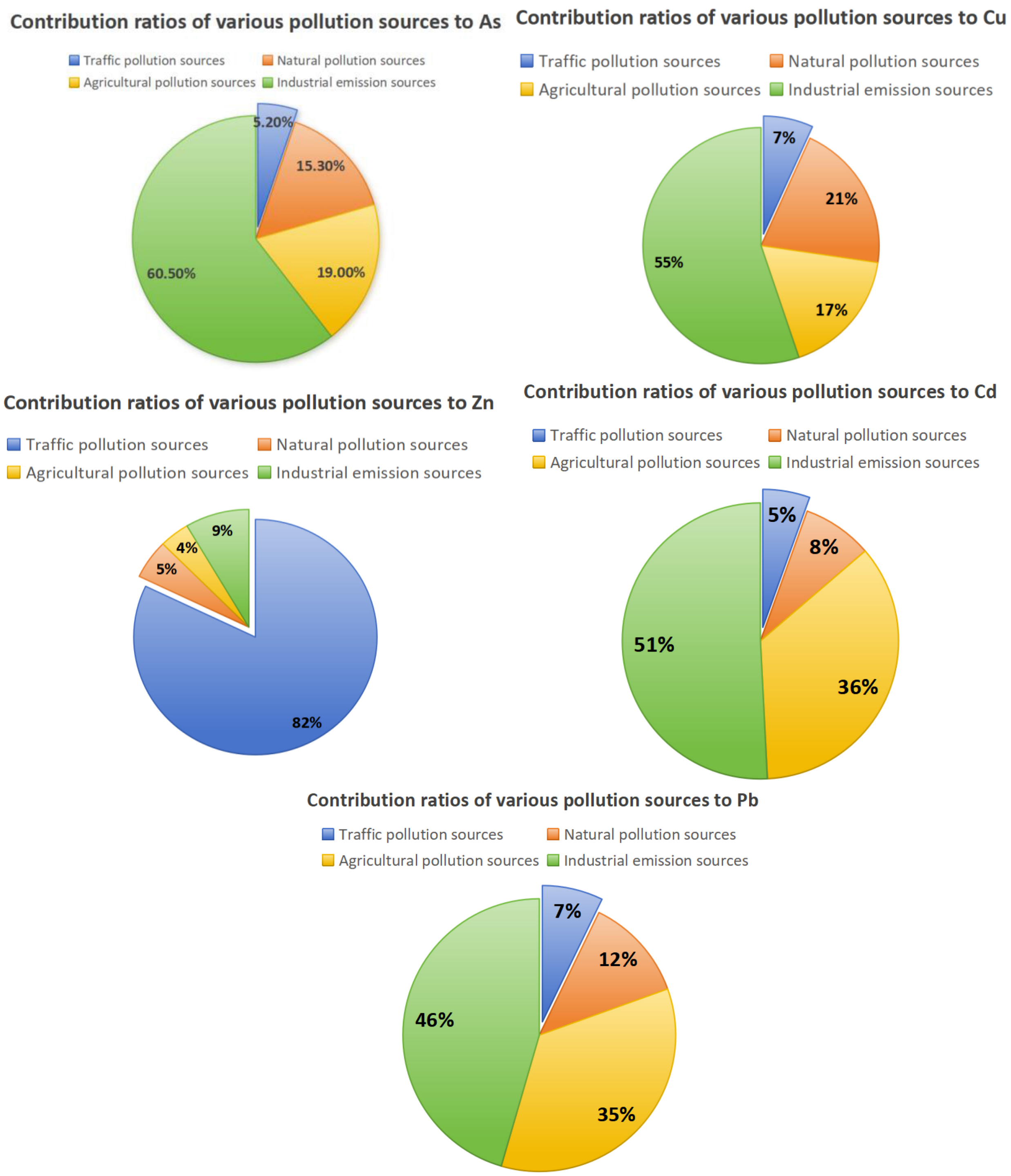

Figure 3. Contribution rates of various pollution sources to each heavy metal.

4. Discussion and Conclusions

4.1. Discussion

4.1.1. Contamination Status and Environmental Implications

This study systematically characterized heavy metal contamination in farmland soils of the Huize mining area. Overall, heavy metals showed varying degrees of accumulation, with Cd being the priority control element: its mean concentration was 1.55 times the Yunnan provincial soil background value, with an exceedance rate of 2.0% against the GB 15618-2018 screening value. In contrast, As, Cu, Zn and Pb mean concentrations were all below the provincial background values, indicating limited overall accumulation at the regional scale.

Notably, the slightly acidic soil conditions (mean pH 5.87) may amplify environmental risks despite relatively low total concentrations (He et al., 2025). Under acidic conditions, heavy metal ions tend to desorb from soil colloids and enter the soil solution, increasing bioavailability and potential for crop uptake (Wang et al., 2025). This is particularly important for Cd, which has high mobility in acidic soils; even moderate total concentrations may pose elevated food safety risks (Song et al., 2025). This finding aligns with previous studies in southwest China's karst regions, where soil acidification has been identified as a key driver of heavy metal activation in both high-background and mining-affected areas (Qin et al., 2022; Sun et al., 2025). This implies that total concentration alone is insufficient for risk assessment in mining areas, and speciation and bioavailability should be incorporated into future risk evaluation frameworks.

4.1.2. Spatial Heterogeneity and Formation Mechanisms

The significant spatial aggregation of heavy metals is jointly controlled by anthropogenic source layouts and natural migration processes. Industrial point sources (mines and smelters) formed core high-value zones for As, Pb, Cd and Cu, showing typical point-source diffusion patterns. Traffic-related Zn formed banded enrichment along main roads, reflecting linear source characteristics (Liang et al., 2025). Agricultural non-point source inputs led to widespread moderate Cd accumulation in cultivation areas.

Beyond source distribution, natural factors also modulate spatial patterns. Precipitation promotes heavy metal leaching and lateral migration, while terrain affects runoff direction and sediment deposition, further reshaping concentration gradients (Wang et al., 2024). Population density, as a proxy for anthropogenic intensity, showed strong correlations with high-concentration zones, indicating that multi-factor interactions amplify spatial heterogeneity (Wu et al., 2026). This is consistent with the consensus that mining-area soil heavy metal distributions result from the coupling of source emission intensity and geochemical migration processes (Li et al., 2022). The geographical detector results further confirm that no single factor can fully explain spatial differentiation, and the interaction between natural and anthropogenic factors exhibits non-linear enhancement effects.

4.1.3. Source Apportionment Reliability and Regional Comparison

The PMF model identified four source categories, with industrial emissions being the dominant source (38.2%), followed by agricultural activities (27.5%), natural background (22.3%) and traffic pollution (12.0%). This source structure is generally consistent with studies of other Pb-Zn mining areas in southwest China, where mining and smelting are universally the primary heavy metal sources. Studies in the Guangxi karst mining area also reported industrial emissions as the largest contributor to Cd and Pb accumulation (Li et al., 2025b).

Compared with purely qualitative source identification methods, the PMF model provides quantitative contribution rates, offering stronger support for precise pollution control (Mu et al., 2024). Combined with spatial distribution analysis, the source apportionment results show good consistency with the actual industrial and agricultural layout of the study area, verifying the reliability of the findings (Jia et al., 2024). It is worth noting that agricultural activities contributed over one-quarter of total heavy metal inputs, which has often been overlooked in previous mining area studies. This highlights the need to consider both industrial point sources and agricultural non-point sources in pollution management.

4.1.4. Control Strategies and Research Limitations

Based on the quantitative source apportionment results and spatial distribution characteristics of soil heavy metals, targeted prevention and control strategies are proposed following the principle of source-specific management and zoned implementation (Zhang et al., 2025). For industrial emissions—the dominant source of As, Cu, Pb and Cd—environmental supervision of mining and smelting enterprises should be tightened, clean production processes widely promoted, and regular soil monitoring coupled with targeted remediation conducted within the 5 km radius of mining and smelting cores, with Cd and Pb designated as priority control elements in core industrial zones (Sui et al., 2025). For traffic pollution that accounts for the vast majority of Zn inputs, transport route planning should be optimized, new-energy vehicles popularized to curb exhaust emissions and tyre wear, and periodic soil remediation performed along major transport corridors with a focus on Zn contamination (Wen et al., 2024). For agricultural non-point source inputs of Cd, Pb and As, green agricultural technologies should be advanced to reduce the use of high-heavy-metal fertilizers and pesticides, and livestock manure application standardized to mitigate agricultural heavy metal inputs (Wan et al., 2024). On this basis, a zoned management scheme is further recommended: comprehensive remediation technologies are applicable to heavily polluted core zones, while crop structure adjustment and agronomic regulation measures are suitable for lightly polluted areas to achieve safe farmland utilization.

This study still has certain limitations. First, the limited number of sampling sites may compromise the accuracy of Kriging interpolation, particularly in the peripheral areas of the study region. Second, the analysis of driving factors does not include soil microbial communities and vegetation coverage, both of which exert important influences on heavy metal migration and transformation in soil environments. Third, the study only captures a snapshot of the current contamination status, without long-term dynamic monitoring of heavy metal accumulation processes and source contribution variations. Looking forward, further research can expand sampling density to improve spatial analysis precision, incorporate heavy metal bioavailability assessment for more scientific risk evaluation, and carry out long-term fixed-point monitoring to reveal the dynamic evolution of heavy metal concentrations and source contributions, thereby providing more solid scientific support for precise soil heavy metal pollution management.

4.2. Conclusions

Farmland soils in the Huize mining area show varying degrees of heavy metal accumulation. Cadmium is the priority contaminant with a mean concentration 1.55 times the Yunnan provincial background value and a 2.0% exceedance rate against the national risk screening value. All elements show high spatial heterogeneity, with coefficients of variation exceeding 0.36.

Heavy metals exhibit significant spatial aggregation. High-concentration zones are concentrated in mining areas, smelter peripheries and major transport routes, while low-value zones occur in remote agricultural and natural areas. Distribution patterns correspond closely to the layout of anthropogenic emission sources.

Four pollution sources were quantitatively identified via the PMF model: industrial emissions (dominant for As, Pb, Cd and Cu, total contribution 38.2%), traffic pollution (dominant for Zn, 12.0%), agricultural activities (27.5%) and natural background (22.3%). Industrial emissions are the primary pollution source in the study area.

Spatial differentiation of heavy metals is driven by the combined effects of natural factors (pH, precipitation, topography) and anthropogenic factors (industrial intensity, traffic, agricultural inputs), with multi-factor interactions amplifying spatial heterogeneity. Targeted zoned control strategies based on source characteristics will support efficient soil pollution management and sustainable agricultural development in the mining area.

Conflicts of Interest

The authors declare no conflicts of interest regarding the publication of this paper.

References

Cheng, X., Chen, Z., Zhou, X., Huang, Q., Shen, J., Chen, Y. et al. (2025). Evaluation of Contamination and Ecological and Health Risk in Surface Soil and Crops Contaminated with Metalloids and Heavy Metals in Datun, China, "the World Tin Capital". *Soil and Sediment Contamination: An International Journal, 34,* 1469-1487. https://doi.org/10.1080/15320383.2024.2435994

Guo, Q., Li, Y., Zheng, L. W., Wei, X. Y., Xu, Y., Shen, Y. W. et al. (2023). Facile Fabrication of Fe/Zr Binary MOFs for Arsenic Removal in Water: High Capacity, Fast Kinetics and Good Reusability. *Journal of Environmental Sciences, 128,* 213-223. https://doi.org/10.1016/j.jes.2022.08.002

He, J., Zhang, H., Yang, K., Li, Y., Bao, L., Gao, L. et al. (2025). Heavy Metal Accumulation Risk and Source Analysis in Soils of Antimony Mining Areas. *Scientific Reports, 15,* Article No. 40010. https://doi.org/10.1038/s41598-025-23789-z

Howlett-Downing, C., Boman, J., Molnár, P., & Wichmann, J. (2026). DN-PMF as a Sensitivity Test for Conventional PMF (C-PMF) Source Apportionment in Three Cities in South Africa, 2017-2018. *Environmental Forensics*. https://doi.org/10.1080/15275922.2026.2628337

Jenkins, E. M., Galbraith, J., & Paltseva, A. A. (2025). Portable X-Ray Fluorescence as a Tool for Urban Soil Contamination Analysis: Accuracy, Precision, and Practicality. *Soil, 11,* 565-582. https://doi.org/10.5194/soil-11-565-2025

Jia, L., Liang, H., Fan, M., Guo, S., Yue, T., Wang, M. et al. (2024). Spatial Distribution and Source Apportionment of Soil Heavy Metals in the Areas Affected by Non-Ferrous Metal Slag Field in Southwest China. *Frontiers in Environmental Science, 12,* Article 1407319. https://doi.org/10.3389/fenvs.2024.1407319

Jomova, K., Alomar, S. Y., Nepovimova, E., Kuca, K., & Valko, M. (2025). Heavy Metals: Toxicity and Human Health Effects. *Archives of Toxicology, 99,* 153-209. https://doi.org/10.1007/s00204-024-03903-2

Kim, N. (2015). The Tangdan Copper Mines and the 1733 Earthquake: A Mining Community before the Boom in the Far Southwest of Qing China. *Cross-Currents: East Asian History and Culture Review, 4,* 285-308. https://doi.org/10.1353/ach.2015.0018

Li, B., Deng, J., Li, Z., Chen, J., Zhan, F., He, Y. et al. (2022). Contamination and Health Risk Assessment of Heavy Metals in Soil and Ditch Sediments in Long-Term Mine Wastes Area. *Toxics, 10,* Article 607. https://doi.org/10.3390/toxics10100607

Li, H., Cui, X., Sun, Y., Zheng, P., Wang, L., & Shi, X. (2025a). Advances in Microbial Remediation of Heavy Metal-Contaminated Soils: Mechanisms, Synergistic Technologies, Field Applications and Future Perspectives. *Toxics, 13,* Article 1069. https://doi.org/10.3390/toxics13121069

Li, Y., Wang, S., Shang, X., Zhou, H., He, J., Chen, W. et al. (2025b). Characterization and Source Apportionment of Heavy Metal Contamination in Agricultural Soils in the Complex Genesis Region of Western Yunnan. *Scientific Reports, 15,* Article No. 32213. https://doi.org/10.1038/s41598-025-16520-5

Liang, N., Zhang, C., Zhang, Y., Jiang, N., Yang, J., Geng, N. et al. (2025). Pollution Levels, Distribution Characteristics and Risk Assessment of Heavy Metals (HMs) in Road Dust in Major Cities of China. *Journal of Hazardous Materials, 494,* Article ID: 138733. https://doi.org/10.1016/j.jhazmat.2025.138733

Liu, Z., Wang, L., Yan, M., Ben Ma,, & Cao, R. (2024). Source Apportionment of Soil Heavy Metals Based on Multivariate Statistical Analysis and the PMF Model: A Case Study of the Nanyang Basin, China. *Environmental Technology & Innovation, 33,* Article ID: 103537. https://doi.org/10.1016/j.eti.2024.103537

Mu, D., Meng, J., Wang, S., Xiao, S., Wang, H., Sun, X. et al. (2024). Source Apportionment, Source-Specific Health Risks, and Control Factors of Heavy Metals in Water Bodies of a Typical Karst Basin in Southwestern China. *PLOS ONE, 19,* e0309142. https://doi.org/10.1371/journal.pone.0309142

Qian, L., Shi, Y., Zheng, L., Xu, X., Xu, Q., Zhou, X. et al. (2025). Assessing Ecological Risks of Soil Heavy Metal Contamination around Diverse Metal Mining Areas in China: From Criteria Derivation to Risk Attribution. *Journal of Cleaner Production, 486,* Article ID: 144536. https://doi.org/10.1016/j.jclepro.2024.144536

Qin, Y., Zhang, F., Xue, S., Ma, T., & Yu, L. (2022). Heavy Metal Pollution and Source Contributions in Agricultural Soils Developed from Karst Landform in the Southwestern

Region of China. *Toxics, 10,* Article 568. https://doi.org/10.3390/toxics10100568

Rajput, P., Singh, A., Mandzhieva, S., Ghazaryan, K., Minkina, T., & Rajput, V. D. (2025). Emerging Remediation Approaches for Mining Contaminated Soils by Heavy Metals: Recent Updates and Future Perspective. *Environmental Geochemistry and Health, 47,* Article No. 255. https://doi.org/10.1007/s10653-025-02553-2

Ren, L., Qi, W., & Ye, H. (2025). Spatial Distribution Characteristics and Risk Assessment of Soil Heavy Metals from Long-Term Mining Activities: A Case Study of the Fengfeng Mining Area. *Toxics, 13,* Article 969. https://doi.org/10.3390/toxics13110969

Song, Y., Wang, J., Ge, Y., & Xu, C. (2020). An Optimal Parameters-Based Geographical Detector Model Enhances Geographic Characteristics of Explanatory Variables for Spatial Heterogeneity Analysis: Cases with Different Types of Spatial Data. *GIScience & Remote Sensing, 57,* 593-610. https://doi.org/10.1080/15481603.2020.1760434

Song, Z., Song, Z., Liu, W., & Lyu, B. (2025). Molecular and Proteomic Analyses of Effects of Cadmium Exposure on the Silk Glands of *Trichonephila clavata*. *International Journal of Molecular Sciences, 26,* Article 754. https://doi.org/10.3390/ijms26020754

Sui, S., Wang, M., Ma, W., Wang, M., Wang, J., Liu, K. et al. (2025). Machine Learning Reveals Heavy Metal Migration Pathways in Asia's Largest Pb-Zn Smelting Region: Soil Pollution Simulation in Jiyuan. *Process Safety and Environmental Protection, 203,* Article ID: 107904. https://doi.org/10.1016/j.psep.2025.107904

Sun, S., Wang, J., Mu, L., Zhang, N., & Bao, L. (2025). Risk Assessment of Heavy Metals in Typical Karst Soils and Analysis of Potential Influencing Factors. *Environmental Geochemistry and Health, 47,* Article No. 244. https://doi.org/10.1007/s10653-025-02555-0

Tan, M., Huang, X. W., Wu, P., & Huang, Z. (2023). Ore-Forming Process of the Huize Super-Large Pb-Zn Deposit, SW China: Constraints from in Situ Elements and S-Pb Isotopes. *Ore Geology Reviews, 159,* Article ID: 105580. https://doi.org/10.1016/j.oregeorev.2023.105580

Wan, Y., Liu, J., Zhuang, Z., Wang, Q., & Li, H. (2024). Heavy Metals in Agricultural Soils: Sources, Influencing Factors, and Remediation Strategies. *Toxics, 12,* Article 63. https://doi.org/10.3390/toxics12010063

Wang, C. C., Zhang, Q. C., Yan, C. A., Tang, G. Y., Zhang, M. Y., Ma, L. Q. et al. (2023). Heavy Metal(loid)s in Agriculture Soils, Rice, and Wheat across China: Status Assessment and Spatiotemporal Analysis. *Science of the Total Environment, 882,* Article ID: 163361. https://doi.org/10.1016/j.scitotenv.2023.163361

Wang, L., Liu, D., Sun, Y., Zhang, Y., Chen, W., Yuan, Y. et al. (2024). Machine Learning-Based Analysis of Heavy Metal Contamination in Chinese Lake Basin Sediments: Assessing Influencing Factors and Policy Implications. *Ecotoxicology and Environmental Safety, 283,* Article ID: 116815. https://doi.org/10.1016/j.ecoenv.2024.116815

Wang, M., Zhang, R., Yan, B., Song, C., Lv, Y., & Zhao, H. (2025). Prediction of Soil Pollution Risk Based on Machine Learning and SHAP Interpretable Models in the Nansi Lake, China. *Toxics, 13,* Article 278. https://doi.org/10.3390/toxics13040278

Wen, M., Ma, Z., Gingerich, D. B., Zhao, X., & Zhao, D. (2022). Heavy Metals in Agricultural Soil in China: A Systematic Review and Meta-Analysis. *Eco-Environment & Health, 1,* 219-228. https://doi.org/10.1016/j.eehl.2022.10.004

Wen, Z. Q., Miao, Q. Y., Chen, J. R., Wu, S. P., He, L. X., Jiang, B. Q. et al. (2024). Heavy Metal Emissions from On-Road Vehicles in Xia-Zhang-Quan Metropolitan Area in Southeastern China from 2015 to 2060: Impact of Vehicle Electrification. *Environmental Science and Pollution Research, 32,* 298-313. https://doi.org/10.1007/s11356-024-35772-8

Wu, Y., Li, X., Yu, L., Wang, T., Wang, J., & Liu, T. (2022). Review of Soil Heavy Metal

Pollution in China: Spatial Distribution, Primary Sources, and Remediation Alternatives. *Resources, Conservation and Recycling, 181,* Article ID: 106261. https://doi.org/10.1016/j.resconrec.2022.106261

Wu, Z., Liu, Y., Zhu, M., Zeng, J., Labat, D., & Meng, F. (2026). SWAT-WASP Coupled Modeling of Ammonia Nitrogen in Rare Earth Mining Watersheds. *Water Science & Technology, 93,* 273-295. https://doi.org/10.2166/wst.2025.190

Xie, H., Shi, Y., Wang, L., Yan, H., Ci, M., Wang, Z. et al. (2024). Source and Risk Assessment of Heavy Metals in Mining-Affected Areas in Jiangxi Province, China, Based on Monte Carlo Simulation. *Environmental Science and Pollution Research, 31,* 21765-21780. https://doi.org/10.1007/s11356-024-32554-0

Xu, L., Zhao, F., Xing, X., Peng, J., Wang, J., Ji, M. et al. (2024). A Review on Remediation Technology and the Remediation Evaluation of Heavy Metal-Contaminated Soils. *Toxics, 12,* Article 897. https://doi.org/10.3390/toxics12120897

Yang, L., Yang, M., Wang, L., Peng, F., Li, Y., & Bai, H. (2018). Heavy Metal Contamination and Ecological Risk of Farmland Soils Adjoining Steel Plants in Tangshan, Hebei, China. *Environmental Science and Pollution Research, 25,* 1231-1242. https://doi.org/10.1007/s11356-017-0551-8

Zhang, Y., Huang, R., & Jiang, B. (2025). Prioritizing Soil Heavy Metal Control Based on Source-Specific Probabilistic Ecological-Health Risk Assessment in Industrial Development Areas of Shouguang, a Typical Agricultural City in China. *Environmental Geochemistry and Health, 47,* Article No. 465. https://doi.org/10.1007/s10653-025-02784-3